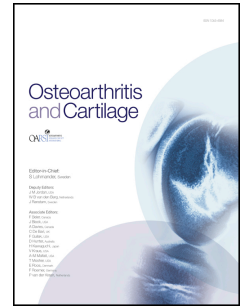


# Journal Pre-proof

Contribution of nerves within osteochondral channels to osteoarthritis knee pain in humans and rats

Koji Aso, Seyed Mohsen Shahtaheri, Roger Hill, Deborah Wilson, Daniel F. McWilliams, Lilian N. Nwosu, Victoria Chapman, David A. Walsh



PII: S1063-4584(20)31026-8

DOI: <https://doi.org/10.1016/j.joca.2020.05.010>

Reference: YJOCA 4674

To appear in: *Osteoarthritis and Cartilage*

Received Date: 4 October 2019

Revised Date: 12 May 2020

Accepted Date: 13 May 2020

Please cite this article as: Aso K, Shahtaheri SM, Hill R, Wilson D, McWilliams DF, Nwosu LN, Chapman V, Walsh DA, Contribution of nerves within osteochondral channels to osteoarthritis knee pain in humans and rats, *Osteoarthritis and Cartilage*, <https://doi.org/10.1016/j.joca.2020.05.010>.

This is a PDF file of an article that has undergone enhancements after acceptance, such as the addition of a cover page and metadata, and formatting for readability, but it is not yet the definitive version of record. This version will undergo additional copyediting, typesetting and review before it is published in its final form, but we are providing this version to give early visibility of the article. Please note that, during the production process, errors may be discovered which could affect the content, and all legal disclaimers that apply to the journal pertain.

© 2020 Osteoarthritis Research Society International. Published by Elsevier Ltd. All rights reserved.

1 **Running title; Osteochondral nerves and osteoarthritis knee pain**

2 **Full title: Contribution of nerves within osteochondral channels to osteoarthritis knee**  
3 **pain in humans and rats**

4  
5 Koji Aso<sup>1,5</sup>, Seyed Mohsen Shahtaheri<sup>1</sup>, Roger Hill<sup>1,2</sup>, Deborah Wilson<sup>1,2</sup>, Daniel F.  
6 McWilliams<sup>1</sup>, Lilian N Nwosu<sup>3</sup>, Victoria Chapman<sup>4</sup>, David A. Walsh<sup>1,2</sup>.

7 1 Arthritis Research UK Pain Centre & NIHR Nottingham Biomedical Research Centre,  
8 School of Medicine, University of Nottingham, NG5 1PB, UK.

9 2 Sherwood Forest Hospitals NHS Foundation Trust, Mansfield, Road, Sutton in Ashfield,  
10 NG17 4JL, UK.

11 3 Musculoskeletal Research Group, Institute of Cellular Medicine, Newcastle University,  
12 NE2 4HH, UK

13 4 Arthritis Research UK Pain Centre, School of Life Sciences, University of Nottingham,  
14 NG7 2UH, UK

15 5 Department of Orthopedic Surgery, Kochi Medical School, Kochi University, 185-1  
16 Oko-cho Kohasu, Nankoku 783-8505, Japan.

17 \*Corresponding author: Koji Aso, MD PhD

18 Department of Orthopedic Surgery

19 Kochi Medical School, Kochi University

20 185-1 Oko-cho Kohasu, Nankoku, JAPAN, 783-8505

21 Email: koji.aso@gmail.com

22 Tel: +81-88-880-2386

23 FAX: +81-88-880-2388

24 ORCID: 0000-0003-3763-9564

25  
26  
27  
28  
29  
30  
31  
32  
33  
34  
35  
36

**37 Abstract****38 Objectives**

39 Subchondral bone may contribute to knee osteoarthritis (OA) pain. Nerve growth factor  
40 (NGF) can stimulate nerve growth through TrkA. We aimed to identify how sensory nerve  
41 growth at the osteochondral junction in human and rat knees associates with OA pain.

**42 Methods**

43 Eleven symptomatic chondropathy cases were selected from people undergoing total knee  
44 replacement for OA. Twelve asymptomatic chondropathy cases who had not presented  
45 with knee pain were selected post-mortem. OA was induced in rat knees by meniscal  
46 transection (MNX) and sham-operated rats were used as controls. Twice-daily oral doses  
47 (30 mg/kg) of TrkA inhibitor (AR786) or vehicle were administered from before and up to  
48 28 days after OA induction. Joints were analysed for macroscopic appearances of articular  
49 surfaces, OA histopathology and calcitonin gene-related peptide-immunoreactive  
50 (CGRP-IR) sensory nerves in medial tibial plateaux, and rats were assessed for pain  
51 behaviors.

**52 Results**

53 The percentage of osteochondral channels containing CGRP-IR nerves in symptomatic  
54 chondropathy was higher than in asymptomatic chondropathy (difference: 2.5% [95% CI:  
55 1.1-3.7]), and in MNX- than in sham-operated rat knees (difference: 7.8% [95%CI:  
56 1.7-15.0]). Osteochondral CGRP-IR innervation was significantly associated with pain  
57 behavior in rats. Treatment with AR786 prevented the increase in CGRP-IR nerves in  
58 osteochondral channels and reduced pain behavior in MNX-operated rats. Structural OA  
59 was not significantly affected by AR786 treatment.

**60 Conclusions**

61 CGRP-IR sensory nerves within osteochondral channels are associated with pain in human  
62 and rat knee OA. Reduced pathological innervation of the osteochondral junction  
63 might contribute to analgesic effects of reduced NGF activity achieved by blocking  
64 TrkA.

65

66

67

68

69

70

71

72

73

74 **Introduction**

75 Knee osteoarthritis (OA) is a common cause of pain and disability. Pain is the most  
76 common reason sufferers seek medical help. Recent human studies showed that  
77 subchondral bone marrow lesions (BMLs) detected on magnetic resonance imaging (MRI)  
78 in knee OA are associated with pain<sup>1-3</sup>. Microarray analysis of subchondral BMLs in OA  
79 demonstrated upregulation of genes implicated in neurogenesis, osteochondral turnover  
80 and inflammation that might contribute to OA pain<sup>4</sup>.

81 Nerve growth factor (NGF) is localized in subchondral bone of the human tibial plateau<sup>5</sup>,  
82 cartilage<sup>5</sup> and synovium<sup>6</sup> in OA and rheumatoid arthritis and NGF plays a key role in the  
83 generation of knee OA pain through actions on its high affinity receptor tropomyosin  
84 receptor kinase A (TrkA). The NGF/TrkA pathway has emerged as an important  
85 therapeutic target for human OA pain. Antibodies that block NGF reduce pain in human  
86 and rodent knee OA<sup>7</sup>, and selective, allosteric inhibitors of TrkA such as AR786 can inhibit  
87 pain in rat OA models<sup>8</sup>, and in human OA<sup>9</sup>, although a randomized controlled trial did not  
88 suggest analgesic effects of TrkA inhibition in knee OA<sup>10</sup>.

89 NGF/TrkA pathway inhibitors reduce pain through direct actions on peripheral sensory  
90 nerves. TrkA is expressed by peptidergic nerves which contain the neuropeptide calcitonin  
91 gene-related peptide (CGRP)<sup>11</sup>. CGRP-immunoreactive (IR) sensory nerves contribute to  
92 OA pain<sup>12, 13</sup>. NGF increases pain by sensitizing nerves<sup>14</sup>. NGF can also stimulate sensory  
93 nerve growth<sup>15, 16</sup>. Sensory nerve densities have been associated with pain in nonhealed  
94 bone fractures<sup>17</sup>, aging bone<sup>18</sup> and breast pain<sup>19</sup>. However it is unclear whether sensory  
95 nerve growth contributes to OA pain and whether NGF/TrkA pathway inhibitors are  
96 effective against pathological sensory innervation in OA. In people with OA, CGRP-IR

97 sensory nerves are colocalized with NGF within osteochondral channels<sup>5</sup>, and increased  
98 NGF expression in osteochondral channels was associated with symptomatic human knee  
99 OA<sup>20</sup>. In this study, CGRP-like immunoreactivity was used as a well-established marker of  
100 unmyelinated sensory nerves to confirm innervation at the osteochondral junction.

101 The first objective of this study was to determine if CGRP-IR sensory nerves at the  
102 osteochondral junction are associated with OA pain in humans by comparing cases with  
103 similar OA structural change but with or without symptoms. One group had sought help for  
104 knee pain and undergone total knee replacement (TKR) surgery (symptomatic  
105 chondropathy), while the other group had not sought help for knee pain but had died from  
106 an unrelated illness (asymptomatic chondropathy). Our second objective was to identify  
107 the effects of blocking NGF activity by inhibiting TrkA on any OA-associated increase of  
108 CGRP-IR sensory nerves and pain behavior in rats with surgically-induced OA. We  
109 hypothesise that lower numbers of CGRP-IR sensory nerves within osteochondral channels,  
110 due either to pathological phenotype or TrkA inhibition, is associated with less OA pain.

111

## 112 **Material and Methods**

### 113 **Human tissues**

114 Eleven symptomatic chondropathy cases were selected from people who had presented  
115 with severe knee pain and had undergone TKR for OA. Twelve asymptomatic  
116 chondropathy cases who had not presented with knee pain and 11 non-arthritic control  
117 cases who had macroscopically normal articular cartilage or only mild chondropathy were  
118 selected post-mortem (PM). One knee joint from each donor was included. All  
119 asymptomatic chondropathy cases had not sought medical attention for knee pain during  
120 the last year and are highly likely to have experienced less pain than the symptomatic

121 chondropathy cases. Human tissues were selected according to predefined criteria from a  
122 human Joint Tissue Repository held by the University of Nottingham containing donations  
123 from >2,500 cases at arthroplasty and >400 cases collected post mortem<sup>21</sup>. Informed  
124 consent was obtained from TKR cases, or from the next of kin of PM cases. Protocols were  
125 approved by Nottingham 1 Research Ethics Committee 05/Q2403/24 and Derby Research  
126 Ethics Committee 1 11/H0405/2. Symptomatic chondropathy samples were from people  
127 fulfilling American College of Rheumatology classification criteria for OA<sup>22</sup> at the time of  
128 TKR.

### 129 **Human sample processing**

130 Formalin-fixed coronal sections of the middle third of medial tibial plateaux - MTP (key  
131 weight-bearing area characteristically affected by OA) were decalcified in 10%  
132 ethylenediaminetetraacetic acid (EDTA) in 10mM Tris buffer (pH 6.95, 4°C) prior to wax  
133 embedding. Samples used for CGRP-IR nerves staining were fixed by the method of  
134 Zamboni<sup>23</sup> (Supplementary text). Zamboni's fixed tissues were decalcified, then immersed  
135 and frozen at an optimal cutting temperature and stored at 80°C.

### 136 **Macroscopic chondropathy score and radiographic OA severity score**

137 Following tissue harvesting, articular surfaces of the MTP were evaluated on the extent  
138 and severity of loss of surface integrity by a single assessor<sup>24</sup>. Articular surface defects  
139 were graded 0 [normal], 1 [swelling and softening], 2 [superficial fibrillation], 3 [deep  
140 fibrillation] and 4 [subchondral bone exposure]. The proportion of articular surface area  
141 corresponding to each grade was allocated to each severity grade to calculate a  
142 macroscopic chondropathy score;

143 Macroscopic chondropathy score (0-100) = (Grade 1 x 0.14) + (Grade 2 x 0.34) + (Grade 3  
144 x 0.65) + Grade 4<sup>24</sup>.

145 Radiographic OA severity scores were derived using preoperative postero-anterior knee  
146 radiographs as previously described<sup>24</sup>. An atlas of line drawings of the knee joint was used  
147 to grade medial and lateral joint space narrowing and osteophytes<sup>25</sup>. Scores for  
148 tibiofemoral joint space narrowing (0–6) and osteophytes (0–12) were summed to provide  
149 a total radiographic OA severity score (0–18)<sup>24</sup>.

### 150 **Human histology and grading**

151 Tibial plateaux sections (5µm) were stained with H&E, or Safranin-O and fast green. OA  
152 articular cartilage changes were graded using the Mankin scoring system<sup>26</sup> (Supplementary  
153 text). Subchondral bone marrow replacement was defined as replacement of bone marrow  
154 fat spaces with fibrovascular tissue, and assessed as either present or absent. Section width  
155 was measured by a digital electronic caliper (Mitutoyo, UK), and densities were calculated  
156 of osteochondral channels per mm in subchondral bone, calcified cartilage and  
157 non-calcified cartilage, and of channels breaching tidemark.

### 158 **Immunohistochemistry and quantification of CGRP-IR nerve**

159 Tibial plateaux sections (20µm) were blocked with 3% bovine serum albumin (BSA) for  
160 1h at room temperature. The sections incubated in mouse anti-CGRP antibody (1:300  
161 TA309091; Acris Antibodies, Herford, Germany) were diluted in goat blocking serum  
162 overnight in a humid chamber at 4°C. The next day, secondary detection was performed  
163 with goat anti-mouse IgG conjugated with Alexa 488 (1:100 A32723; ThermoFisher  
164 scientific, Mississippi, USA) for CGRP for 2h at room temperature. Before, between, and  
165 after each incubation step, the sections were washed three times for 5min in PBS.  
166 CGRP-IR sensory nerves were measured as a proportion (%) of osteochondral channels in  
167 each case that displayed CGRP-IR sensory nerves. One section per each knee joint was  
168 used for analysis of CGRP-IR nerves.

**169 Animals and OA induction**

170 Male Sprague-Dawley rat knee joints (Charles River, Kent, UK), n=30, were collected for  
171 this study from our previous experiment<sup>8</sup>. The rats were used in accordance with UK Home  
172 Office regulations and followed the guidelines of the International Association for the  
173 Study of Pain. Rats weighing 200–250 g were anaesthetized briefly with isoflurane (2% in  
174 O<sub>2</sub>) and underwent transection of the medial meniscus (MNX; n=20)<sup>27</sup>. Non-osteoarthritic  
175 (Sham-operated; n=10) rats were used as controls. Rats were randomized to 3 groups  
176 (sham plus vehicle, MNX plus vehicle and MNX plus AR786) using a computer program,  
177 and mixed within cages. Data presented in this paper extend behavioural data and  
178 macroscopic chondropathy scores that have been reported previously from these rats<sup>8</sup>. All  
179 outcome measurements were carried out by an experimenter blinded to randomized  
180 treatments.

**181 TrkA inhibitor (AR786) administration**

182 AR786 (Array Biopharma, Boulder, Colorado, USA) was administered in a preventive  
183 protocol based on previous data<sup>28, 29</sup>. Oral doses (30 mg/kg) of AR786 or vehicle (5%  
184 Gelucire 50/13) were administered 1h prior to and 8h following OA induction, and twice  
185 daily until the end of the study (28 days after OA induction).

**186 Rat knee joint pathology and quantification of CGRP-IR nerve**

187 Rats were sacrificed by an overdose of pentobarbital (intraperitoneal) (day 28). Macroscopic  
188 chondropathy scores based on the Guingamp classification<sup>30</sup> have been previously published<sup>8</sup>. For  
189 the current report, histological assessment of cartilage and subchondral bone including osteophytes  
190 in medial tibial plateaux was undertaken based on the Osteoarthritis Research Society  
191 International recommendations<sup>31</sup>. Subchondral bone marrow replacement by fibrovascular  
192 tissue and osteochondral channel density were assessed in the same way as human samples.



193 Immunohistochemistry and quantification of CGRP-IR nerve fibers in osteochondral  
194 channels in medial tibial plateaux were carried out in the same way as human samples.  
195 Width of the entire medial proximal tibial epiphysis was measured by a digital caliper and  
196 CGRP-IR nerve density per mm in the bone marrow space was calculated. Two sections  
197 containing weight-bearing area characteristically affected by OA per each knee joint were  
198 used for analysis of CGRP-IR nerves.

### 199 **Behavioral measurements of OA pain**

200 Pain behavior was assessed as weight-bearing asymmetry and as paw withdrawal threshold  
201 to punctate stimulation of the hind-paw. Baseline measurements were obtained  
202 immediately prior to intra-articular injection or surgery (day 0) and every 2–4 days from  
203 day 3 onwards to day 28 and have been previously reported<sup>8</sup>. Weight-bearing asymmetry  
204 was assessed as percent difference in weight distribution between hind-limbs<sup>32</sup>.

### 205 **Image analysis**

206 All human and rat histological scoring and quantification of CGRP-IR nerve fibers were  
207 undertaken by a single observer (KA) who was blinded to the diagnostic group, using a  
208 Zeiss Axioscop-50 microscope (Carl Zeiss, Welwyn Garden City, UK).

### 209 **Statistical analysis**

210 Statistical analyses were performed with JMP, Version 10 (SAS Ins. Cary, NC), IBM SPSS  
211 version 26.0 software and IBM SPSS Bootstrapping (IBM Corp. Armonk, NY, USA). Data  
212 of age, gender, radiographic OA score, macroscopic chondropathy score, OA  
213 histopathology, CGRP sensory nerve and pain behaviours were analyzed using  
214 Kruskal-Wallis tests followed by post hoc Dunn's comparisons. Estimates of mean  
215 differences of CGRP-IR nerve between groups with 95% confidence interval (CI) were  
216 derived from 2000 bootstrap resampling. Logistic regression was performed to adjust for

217 age. Spearman's rank correlation ( $r$ ) assessed associations between pain behaviors and  
218 CGRP-IR nerve densities, macroscopic chondropathy score and OA istological changes in  
219 MNX plus vehicle and MNX plus AR786 models ( $n=20$ ). The 95% CIs for Spearman's  
220 correlation were derived from 2000 bootstrap resampling. Bias-corrected and accelerated  
221 percentile method were used for estimation of CIs.  $P<0.05$  indicated statistical  
222 significance.

223

## 224 **Results**

### 225 **Patient characteristics and joint pathology**

226 Demographics and sample details of cases selected for this study are shown in Table 1. The  
227 asymptomatic chondropathy group was older than the non-arthritic control and  
228 symptomatic chondropathy groups. As expected from our selection criteria,  
229 macroscopic chondropathy scores were similar in asymptomatic and symptomatic  
230 chondropathy groups; and both were higher than in non-arthritic controls. Histological  
231 chondropathy scores were higher in chondropathy cases than in non-arthritic controls  
232 (Table 1 and Figure 1 A, B, C). Channels were present at the osteochondral junction in  
233 each group (Figure 1, D). Increased numbers of osteochondral channels breaching the  
234 tidemark (Figure 1 E), and the percentage of cases with subchondral bone marrow  
235 replacement by fibrovascular tissue did not reach statistical significance in chondropathy  
236 groups compared to non-arthritic controls (Table 1).

### 237 **CGRP-IR sensory nerve fibers in human medial tibial plateaux**

238 CGRP-IR nerve profiles were localized to osteochondral channels and subchondral bone  
239 marrow spaces (Figure 1 F, G, H). The percentage of osteochondral channels containing  
240 CGRP-IR sensory nerves did not significantly differ between chondropathy and

241 non-arthritic control groups (median percentages (interquartile range (IQR)) of  
242 non-arthritic control, asymptomatic and symptomatic chondropathy were 1.2 (0, 2.9), 0 (0,  
243 1.9) and 3.6 (2.5, 4.7)) (Figure 2). Bootstrap estimates of mean differences between  
244 asymptomatic or symptomatic chondropathy and non-arthritic control were 0.8% [95% CI:  
245 -0.6 to 2.4%] and 1.3% [95%CI: -0.4 to 2.9%], respectively. The percentage of  
246 osteochondral channels containing CGRP-IR sensory nerves in the symptomatic  
247 chondropathy group was higher than in asymptomatic chondropathy group and this  
248 difference remained significant after adjusting for age (aOR=3.9 [95% CI: 1.5 to 31.3],  
249 p=0.01) (Figure 2). The bootstrap estimate of mean difference between symptomatic and  
250 asymptomatic chondropathy was 2.5% [95% CI: 1.1 to 3.7%].

#### 251 **MNX-induced OA and pain behavior in rats**

252 New data presented here extend previously published macroscopic chondropathy scores,  
253 paw withdrawal thresholds and weight-bearing asymmetry data from these experiments.<sup>8</sup>  
254 MNX surgery was associated with a greater OA structural change than was sham surgery  
255 (Table 2 and Figure 3A, B, C). Subchondral bone marrow replacement by fibrovascular  
256 tissue was observed in MNX- but not in sham-operated rats. Numbers of osteochondral  
257 channels did not differ between groups, and were not altered by AR786 treatment (Table 2  
258 and Figure 3D, E, F, C). Asymmetric weight distribution and reduced paw withdrawal  
259 thresholds were more severe in MNX-operated rats treated with vehicle than in  
260 sham-operated rats at day 28 after surgery, and AR786 reversed the OA-induced pain  
261 behavior (Table 2).

#### 262 **CGRP-IR nerve fibers in rat knee joints**

263 CGRP-IR nerve profiles were localized to osteochondral channels and subchondral bone  
264 marrow spaces in rat knee joints (Figure 3G, H, K). The percentage of osteochondral

265 channels containing CGRP-IR sensory nerves was higher in MNX-operated knees from  
266 rats treated with vehicle than in sham-operated knees (median percentages (IQR) of sham  
267 plus vehicle and MNX plus vehicle were 2.8 (0.5, 7.4) and 10 (8, 13.7)) (Figure 4A). The  
268 bootstrap estimate of mean difference between sham plus vehicle and MNX plus vehicle  
269 was 7.8% [95% CI: 1.7 to 15.0%]. Treatment with AR786 prevented this increase (Figure  
270 4A and Figure 3G, H, I, J). The bootstrap estimate of mean difference between MNX plus  
271 vehicle and MNX plus AR786 groups was 7.7% [95% CI: 2.5 to 14.4%]. CGRP-IR  
272 sensory nerve density in subchondral bone marrow spaces did not differ between groups  
273 (Figure 4B). The percentage of osteochondral channels containing CGRP-IR sensory  
274 nerves in knees from rats 28 days after MNX surgery, treated with vehicle or AR786, was  
275 significantly associated with weight-bearing asymmetry (Spearman's  $r=0.50$  [95% CI: 0.07  
276 to 0.77],  $p=0.04$ ), and with paw withdrawal threshold (Spearman's  $r=-0.55$  [95% CI: -0.82  
277 to -0.08],  $p=0.02$ ).

278

## 279 Discussion

280 We have identified CGRP-IR sensory nerves within osteochondral channels, associated  
281 with symptoms in human knee OA and pain behaviour in MNX-induced rat knee OA.  
282 These new data support the view that CGRP-IR sensory nerves invade the osteochondral  
283 channels from bone marrow spaces in joints with OA cartilage damage. In rats, blocking  
284 NGF activity by inhibiting TrkA prevented the OA-induced growth of CGRP-IR sensory  
285 nerves in osteochondral channels. This was associated with, and might contribute to,  
286 reduced pain behaviour. Our findings support the hypothesis that NGF-induced growth of  
287 sensory nerves at the osteochondral junction might contribute to chronic pain in knee OA.

288 In our previous studies on human tissues, we showed NGF-like immunoreactivity in

289 multinucleate osteoclasts adherent to bone, osteochondral channels and synovium (but not  
290 mRNA expression) was associated with OA pain in human OA<sup>20,6,33</sup>. In the mouse OA  
291 model induced by destabilization of the medial meniscus, increased NGF messenger RNA  
292 in knee joints was also associated with pain behavior<sup>34</sup>. Increased NGF expression by  
293 osteoclasts might induce the invasion by CGRP-IR sensory nerves into osteochondral  
294 channels. Indeed, nerve fibers are increased in channels under areas of most damaged  
295 articular cartilage in osteoarthritic mouse knees<sup>35</sup>, and chondrocytes produce higher NGF  
296 levels in more severely damaged cartilage in human OA<sup>36,37,38</sup> and in surgically-induced  
297 mouse knee OA<sup>39</sup>. However, chondrocyte-derived NGF was not significantly associated  
298 with pain in late-stage OA<sup>20</sup>. These findings suggest a more important contribution to the  
299 generation of pain from NGF in osteochondral channels and synovium than from  
300 chondrocytes, particularly in late-stage OA. Here we demonstrate that inhibition of the  
301 NGF/TrkA pathway with a specific TrkA inhibitor reduced osteochondral innervation in  
302 the rat. These data extend previous findings that NGF-blocking antibodies can reduce  
303 pathological sensory innervation in bone<sup>40</sup> or skin<sup>41</sup>, to show similar effects of TrkA  
304 inhibition in osteochondral channels. NGF pathway inhibition did not, however, have  
305 detectable effects on mature sensory innervation, consistent with a lack of effect on mature  
306 innervation in other tissues from NGF-blockade<sup>42</sup>. Subchondral bone marrow lesions  
307 detected by MRI have been associated with OA pain<sup>1-3</sup>. We speculate that sensitization of  
308 pre-existing nerves in subchondral bone marrow lesions might contribute to OA pain, and  
309 that generation of neurotrophic factors by BMLs<sup>4</sup> might contribute to osteochondral  
310 channel innervation.

311 Nerve growth into articular cartilage occurs within vascular channels. Penetration of  
312 channels into non-calcified articular cartilage has been associated previously with OA

313 disease, whereas total osteochondral channel densities in calcified and non-calcified  
314 cartilage differ little between OA and non-arthritic joints<sup>5</sup>. We found that CGRP-IR sensory  
315 nerve densities within osteochondral channels (but not osteochondral channel densities per  
316 se) were higher in symptomatic than in asymptomatic chondropathy. Also, channel  
317 innervation was significantly associated with weight-bearing asymmetry and paw  
318 withdrawal threshold in MNX-induced rat knee OA. These data suggest that rather than an  
319 increase in osteochondral channel densities, increased innervation contributes to OA pain.  
320 Increased NGF expression in osteochondral channels associated with symptomatic knee  
321 OA<sup>20</sup>, might further contribute to OA pain by sensitizing these osteochondral nerves.

322 As previously reported<sup>8</sup>, blocking NGF activity by oral administration of the specific  
323 TrkA inhibitor AR786 prevented OA-associated pain behaviours in these rats. Inhibiting  
324 the NGF/TrkA pathway reduces peripheral sensitization<sup>43,44</sup>. We now also show that  
325 AR786 administration prevented the increase in CGRP-IR nerves within osteochondral  
326 channels that otherwise follows OA induction by MNX surgery, and that lower CGRP-IR  
327 nerve densities were significantly associated with less OA-induced pain behavior.

328 OA is a multi-tissue disease involving many molecular mediators. Our cross sectional  
329 data from humans, and interventional studies in rats, suggest a contribution of NGF  
330 pathway-induced osteochondral innervation to OA pain. Further research should  
331 investigate whether osteochondral innervation might be a predominant cause of pain in  
332 some patients, and its relative importance compared to other pain mechanisms. CGRP-IR  
333 sensory nerves have also been localized to osteoarthritic synovium<sup>45, 46</sup>, possibly in higher  
334 densities than in asymptomatic knees<sup>47</sup>, particularly in joint compartments displaying  
335 increased sensitivity<sup>45</sup>. Synovitis has also been associated with OA knee pain, both in  
336 humans<sup>6</sup> and in the MNX-induced rat model<sup>48</sup>. However, we previously showed that

337 AR786 did not significantly reduce either knee swelling or synovitis in rats with  
338 MNX-induced OA, and synovitis scores were not significantly associated with pain  
339 behaviors<sup>8</sup>. Other aspects of osteochondral pathology in OA might additionally contribute  
340 to OA pain. Loss of osteochondral integrity might increase osteochondral permeability,  
341 exposing subchondral nerves to chemical mediators from the cartilage or synovium and  
342 mechanical injury<sup>49</sup>. Osteoclast activity may also increase pain both by sensitizing  
343 osteochondral nerves and by increasing structural pathology<sup>50</sup>. Furthermore, NGF both  
344 influences nerve growth, as indicated by our findings, and quickly induces sensitization of  
345 peripheral nerves by multiple signalling pathways<sup>14</sup>. The rapid onset of analgesia  
346 associated with NGF blockade<sup>15</sup> or TrkA inhibition is likely attributable to reduced  
347 peripheral sensitization, rather than to reduced nerve growth, which is a slow process  
348 occurring over a period of weeks<sup>51</sup>. However, our data indicate that osteochondral  
349 innervation might contribute to OA pain, and suggest that nerve growth might be a key  
350 target for structural disease modification in OA. Other approaches for structural disease  
351 modification in OA have been largely unsuccessful, in part due to the prolonged treatment  
352 required to demonstrate clinically important structural modification, and a lack of  
353 symptomatic benefit. Targeting aspects of OA structural pathology such as aberrant  
354 osteochondral innervation with treatments that also more immediately reduce pain is an  
355 attractive proposition.

### 356 ***Limitations***

357 Quantification of nerves is limited by sensitivity of the immunohistochemical method, and  
358 by the challenge of detecting changes in nerve density in a tissue which normally contains  
359 nerves. CGRP-IR was used as a well-established marker of unmyelinated sensory nerves  
360 which express TrkA<sup>11</sup>. Half of neurons innervating the subchondral bone expressed CGRP

361 and TrkA in normal rat knees, whereas all were isolectin B4-negative<sup>52</sup>. Sensitivity of  
362 CGRP to detect subchondral sensory nerves might be even higher in OA<sup>53</sup>. It is unclear  
363 whether CGRP is itself important for OA pain, and, unlike experience with NGF-blocking  
364 antibodies, an RCT of CGRP receptor blockade did not reveal clinically important benefit  
365 for OA pain<sup>54</sup>. However, different results might have been obtained using other neuronal  
366 markers, and we do not exclude biologically important changes in innervation in tissue  
367 compartments additional to osteochondral channels. We used non-parametric statistical  
368 methods in order to optimize validity despite inclusion of an outlying value for channel  
369 innervation in our per protocol analysis. Future research should seek to confirm our present  
370 findings.

371 Characteristics other than osteochondral innervation, some unmeasured, might explain  
372 symptomatic and asymptomatic chondropathy classification. However, the groups had  
373 similar chondropathy scores and OA histopathology. Ageing might also influence sensory  
374 innervation in mice<sup>35,55</sup>, although differences in osteochondral innervation in our study  
375 persisted after adjustment for age. Some people in our 'asymptomatic' chondropathy group  
376 might have experienced chronic knee pain without their relatives knowing. However, all  
377 people undertaking TKR report severe knee pain, and it is highly likely that people who  
378 have not undergone surgery have less knee pain than those who do. Samples were from the  
379 mid-coronal section of the medial tibial plateau, a key weight-bearing area with the  
380 greatest amount of cartilage loss, but findings could differ for other joint regions such as  
381 femoral condyles. We here focused on NGF at the osteochondral junction, and further  
382 systematic studies of other molecules and in other articular tissues might reveal additional  
383 pathways contributing to OA pain.

384 ***Conclusions***



385 Our data indicate a possible role of osteochondral innervation and TrkA in structural  
386 pathology which contributes to OA pain. Previous attempts at structural disease  
387 modification in OA have focused on radiographic features such as joint space narrowing  
388 and osteophytosis, features which are only weakly associated with OA pain severity<sup>56</sup>.  
389 Osteochondral innervation might be a key structural change that contributes to human and  
390 rat OA pain. Most analgesic drugs alter sensory nerve function rather than structure.  
391 Inhibiting pathological nerve growth in osteochondral channels may reduce chronic OA  
392 pain and herald a step change for structural pain modification.

393

#### 394 **Acknowledgements**

395 We express our sincere gratitude to all patients who participated in this study. We would  
396 also like to thank to Karyn S. Bouhana, Steven W. Andrews and colleagues from Array  
397 BioPharma (Colorad, USA) for providing the compounds (AR786 and Gelucire 50/13  
398 vehicle), and Hajime Kuroiwa (Kochi Medical School) for assistance in statistical analysis.

#### 399 **Funding sources**

400 This study was supported by a grant from Versus Arthritis (Centre initiative grant number  
401 18769 and 20777) and a grant from Japanese Orthopaedic Society Knee, Arthroscopy and  
402 Sports Medicine, 2016.

#### 403 **Author Contributions**

404 All authors approved the final version to be published. K.A. had full access to all of the  
405 data in the study and takes responsibility for the integrity of the data and the accuracy of  
406 the data analysis. K.A., D.M., L.N., V.C. and D.W. designed the experiments, analyzed and  
407 interpreted results, and wrote the manuscript. K.A. and M.S. did immunohistochemistry,  
408 histological analysis. R. H. and D. W. did human sample processing. L.N. did pain-related  
409 behavior tests and macroscopic chondropathy scoring in rats. K.A., D.M. and D.W.  
410 analyzed and interpreted the results.

#### 411 **Ethics approval**

412 Nottingham 1 Research Ethics Committee [05/Q2403/24] and Derby Research Ethics  
413 Committee 1 [11/H0405/2].

#### 414 **Conflict of interest**

415 D.A. Walsh: Grants from Arthritis Research UK, while the study was being conducted;  
416 grants from Pfizer Ltd, other from Pfizer Ltd, personal fees from GlaxoSmithKline, outside

417 the submitted work.

418 D. F. McWilliams: grants from Pfizer Ltd.

419 The remaining authors have no conflicts of interest to declare.

Journal Pre-proof

## References

1. Zhang Y, Nevitt M, Niu J, Lewis C, Torner J, Guermazi A, et al. Fluctuation of knee pain and changes in bone marrow lesions, effusions, and synovitis on magnetic resonance imaging. *Arthritis Rheum* 2011; 63: 691-9.
2. Felson DT, Niu J, Guermazi A, Roemer F, Aliabadi P, Clancy M, et al. Correlation of the development of knee pain with enlarging bone marrow lesions on magnetic resonance imaging. *Arthritis Rheum* 2007; 56: 2986-92.
3. Felson DT, Chaisson CE, Hill CL, Totterman SM, Gale ME, Skinner KM, et al. The association of bone marrow lesions with pain in knee osteoarthritis. *Ann Intern Med* 2001; 134: 541-9.
4. Kuttapitiya A, Assi L, Laing K, Hing C, Mitchell P, Whitley G, et al. Microarray analysis of bone marrow lesions in osteoarthritis demonstrates upregulation of genes implicated in osteochondral turnover, neurogenesis and inflammation. *Ann Rheum Dis* 2017; 76: 1764-73.
5. Walsh DA, McWilliams DF, Turley MJ, Dixon MR, Franses RE, Mapp PI, et al. Angiogenesis and nerve growth factor at the osteochondral junction in rheumatoid arthritis and osteoarthritis. *Rheumatology (Oxford)* 2010; 49: 1852-61.
6. Stoppiello LA, Mapp PI, Wilson D, Hill R, Scammell BE, Walsh DA. Structural associations of symptomatic knee osteoarthritis. *Arthritis Rheumatol* 2014; 66: 3018-27.
7. Xu L, Nwosu LN, Burston JJ, Millns PJ, Sagar DR, Mapp PI, et al. The anti-NGF antibody muMab 911 both prevents and reverses pain behaviour and subchondral osteoclast numbers in a rat model of osteoarthritis pain. *Osteoarthritis Cartilage* 2016; 24: 1587-95.
8. Nwosu LN, Mapp PI, Chapman V, Walsh DA. Blocking the tropomyosin receptor kinase A (TrkA) receptor inhibits pain behaviour in two rat models of osteoarthritis. *Ann Rheum Dis* 2016; 75: 1246-54.
9. Krupka E, Jiang GL, Jan C. Efficacy and safety of intra-articular injection of tropomyosin receptor kinase A inhibitor in painful knee osteoarthritis: a randomized, double-blind and placebo-controlled study. *Osteoarthritis Cartilage* 2019.
10. Watt FE, Blauwet MB, Fakhoury A, Jacobs H, Smulders R, Lane NE. Tropomyosin-related kinase A (TrkA) inhibition for the treatment of painful knee osteoarthritis: results from a randomized controlled phase 2a trial. *Osteoarthritis Cartilage* 2019.
11. Averill S, McMahon SB, Clary DO, Reichardt LF, Priestley JV. Immunocytochemical localization of trkA receptors in chemically identified subgroups of adult rat sensory

- neurons. *Eur J Neurosci* 1995; 7: 1484-94.
12. Walsh DA, McWilliams DF. CGRP and Painful Pathologies Other than Headache. *Handb Exp Pharmacol* 2019; 255: 141-67.
  13. Ferreira-Gomes J, Adaes S, Sarkander J, Castro-Lopes JM. Phenotypic alterations of neurons that innervate osteoarthritic joints in rats. *Arthritis Rheum* 2010; 62: 3677-85.
  14. Hirth M, Rukwied R, Gromann A, Turnquist B, Weinkauf B, Francke K, et al. Nerve growth factor induces sensitization of nociceptors without evidence for increased intraepidermal nerve fiber density. *Pain* 2013; 154: 2500-11.
  15. Mantyh PW, Koltzenburg M, Mendell LM, Tive L, Shelton DL. Antagonism of nerve growth factor-TrkA signaling and the relief of pain. *Anesthesiology* 2011; 115: 189-204.
  16. Mearow KM. The effects of NGF and sensory nerve stimulation on collateral sprouting and gene expression in adult sensory neurons. *Exp Neurol* 1998; 151: 14-25.
  17. Chartier SR, Thompson ML, Longo G, Fealk MN, Majuta LA, Mantyh PW. Exuberant sprouting of sensory and sympathetic nerve fibers in nonhealed bone fractures and the generation and maintenance of chronic skeletal pain. *Pain* 2014; 155: 2323-36.
  18. Jimenez-Andrade JM, Mantyh WG, Bloom AP, Freeman KT, Ghilardi JR, Kuskowski MA, et al. The effect of aging on the density of the sensory nerve fiber innervation of bone and acute skeletal pain. *Neurobiol Aging* 2012; 33: 921-32.
  19. Gopinath P, Wan E, Holdcroft A, Facer P, Davis JB, Smith GD, et al. Increased capsaicin receptor TRPV1 in skin nerve fibres and related vanilloid receptors TRPV3 and TRPV4 in keratinocytes in human breast pain. *BMC Womens Health* 2005; 5: 2.
  20. Aso K, Shahtaheri SM, Hill R, Wilson D, McWilliams DF, Walsh DA. Associations of symptomatic knee OA with histopathologic features in subchondral bone. *Arthritis Rheumatol* 2019.
  21. Walsh DA, Wilson D. Post-mortem collection of human joint tissues for research. *Rheumatology (Oxford)* 2003; 42: 1556-8.
  22. Altman R, Asch E, Bloch D, Bole G, Borenstein D, Brandt K, et al. Development of criteria for the classification and reporting of osteoarthritis. Classification of osteoarthritis of the knee. Diagnostic and Therapeutic Criteria Committee of the American Rheumatism Association. *Arthritis Rheum* 1986; 29: 1039-49.
  23. Stefanini M, De Martino C, Zamboni L. Fixation of ejaculated spermatozoa for electron microscopy. *Nature* 1967; 216: 173-4.
  24. Walsh DA, Yousef A, McWilliams DF, Hill R, Hargin E, Wilson D. Evaluation of a Photographic Chondropathy Score (PCS) for pathological samples in a study of inflammation in tibiofemoral osteoarthritis. *Osteoarthritis Cartilage* 2009; 17: 304-12.
  25. Nagaosa Y, Mateus M, Hassan B, Lanyon P, Doherty M. Development of a logically

- devised line drawing atlas for grading of knee osteoarthritis. *Ann Rheum Dis* 2000; 59: 587-95.
26. Mankin HJ, Dorfman H, Lippiello L, Zarins A. Biochemical and metabolic abnormalities in articular cartilage from osteo-arthritic human hips. II. Correlation of morphology with biochemical and metabolic data. *J Bone Joint Surg Am* 1971; 53: 523-37.
  27. Mapp PI, Avery PS, McWilliams DF, Bowyer J, Day C, Moores S, et al. Angiogenesis in two animal models of osteoarthritis. *Osteoarthritis Cartilage* 2008; 16: 61-9.
  28. Ghilardi JR, Freeman KT, Jimenez-Andrade JM, Mantyh WG, Bloom AP, Kuskowski MA, et al. Administration of a tropomyosin receptor kinase inhibitor attenuates sarcoma-induced nerve sprouting, neuroma formation and bone cancer pain. *Mol Pain* 2010; 6: 87.
  29. Ghilardi JR, Freeman KT, Jimenez-Andrade JM, Mantyh WG, Bloom AP, Bouhana KS, et al. Sustained blockade of neurotrophin receptors TrkA, TrkB and TrkC reduces non-malignant skeletal pain but not the maintenance of sensory and sympathetic nerve fibers. *Bone* 2011; 48: 389-98.
  30. Guingamp C, Gegout-Pottie P, Philippe L, Terlain B, Netter P, Gillet P. Mono-iodoacetate-induced experimental osteoarthritis: a dose-response study of loss of mobility, morphology, and biochemistry. *Arthritis Rheum* 1997; 40: 1670-9.
  31. Gerwin N, Bendele AM, Glasson S, Carlson CS. The OARSI histopathology initiative - recommendations for histological assessments of osteoarthritis in the rat. *Osteoarthritis Cartilage* 2010; 18 Suppl 3: S24-34.
  32. Bove SE, Calcaterra SL, Brooker RM, Huber CM, Guzman RE, Juneau PL, et al. Weight bearing as a measure of disease progression and efficacy of anti-inflammatory compounds in a model of monosodium iodoacetate-induced osteoarthritis. *Osteoarthritis Cartilage* 2003; 11: 821-30.
  33. Wyatt LA, Nwosu LN, Wilson D, Hill R, Spendlove I, Bennett AJ, et al. Molecular expression patterns in the synovium and their association with advanced symptomatic knee osteoarthritis. *Osteoarthritis Cartilage* 2019; 27: 667-75.
  34. McNamee KE, Burleigh A, Gompels LL, Feldmann M, Allen SJ, Williams RO, et al. Treatment of murine osteoarthritis with TrkAd5 reveals a pivotal role for nerve growth factor in non-inflammatory joint pain. *Pain* 2010; 149: 386-92.
  35. Obeidat AM, Miller RE, Miller RJ, Malfait AM. The nociceptive innervation of the normal and osteoarthritic mouse knee. *Osteoarthritis Cartilage* 2019; 27: 1669-79.
  36. Sato T, Konomi K, Yamasaki S, Aratani S, Tsuchimochi K, Yokouchi M, et al. Comparative analysis of gene expression profiles in intact and damaged regions of

- human osteoarthritic cartilage. *Arthritis Rheum* 2006; 54: 808-17.
37. Blaney Davidson EN, van Caam AP, Vitters EL, Bennink MB, Thijssen E, van den Berg WB, et al. TGF-beta is a potent inducer of Nerve Growth Factor in articular cartilage via the ALK5-Smad2/3 pathway. Potential role in OA related pain? *Osteoarthritis Cartilage* 2015; 23: 478-86.
  38. Iannone F, De Bari C, Dell'Accio F, Covelli M, Patella V, Lo Bianco G, et al. Increased expression of nerve growth factor (NGF) and high affinity NGF receptor (p140 TrkA) in human osteoarthritic chondrocytes. *Rheumatology (Oxford)* 2002; 41: 1413-8.
  39. Driscoll C, Chanalaris A, Knights C, Ismail H, Sacitharan PK, Gentry C, et al. Nociceptive Sensitizers Are Regulated in Damaged Joint Tissues, Including Articular Cartilage, When Osteoarthritic Mice Display Pain Behavior. *Arthritis Rheumatol* 2016; 68: 857-67.
  40. Jimenez-Andrade JM, Bloom AP, Stake JI, Mantyh WG, Taylor RN, Freeman KT, et al. Pathological sprouting of adult nociceptors in chronic prostate cancer-induced bone pain. *J Neurosci* 2010; 30: 14649-56.
  41. Takano N, Sakurai T, Kurachi M. Effects of anti-nerve growth factor antibody on symptoms in the NC/Nga mouse, an atopic dermatitis model. *J Pharmacol Sci* 2005; 99: 277-86.
  42. Sevcik MA, Ghilardi JR, Peters CM, Lindsay TH, Halvorson KG, Jonas BM, et al. Anti-NGF therapy profoundly reduces bone cancer pain and the accompanying increase in markers of peripheral and central sensitization. *Pain* 2005; 115: 128-41.
  43. Miller RE, Block JA, Malfait AM. Nerve growth factor blockade for the management of osteoarthritis pain: what can we learn from clinical trials and preclinical models? *Curr Opin Rheumatol* 2017; 29: 110-18.
  44. Shang X, Wang Z, Tao H. Mechanism and therapeutic effectiveness of nerve growth factor in osteoarthritis pain. *Ther Clin Risk Manag* 2017; 13: 951-56.
  45. Saito T, Koshino T. Distribution of neuropeptides in synovium of the knee with osteoarthritis. *Clin Orthop Relat Res* 2000: 172-82.
  46. Eitner A, Pester J, Nietzsche S, Hofmann GO, Schaible HG. The innervation of synovium of human osteoarthritic joints in comparison with normal rat and sheep synovium. *Osteoarthritis Cartilage* 2013; 21: 1383-91.
  47. Saxler G, Loer F, Skumavec M, Pfortner J, Hanesch U. Localization of SP- and CGRP-immunopositive nerve fibers in the hip joint of patients with painful osteoarthritis and of patients with painless failed total hip arthroplasties. *Eur J Pain* 2007; 11: 67-74.
  48. Mapp PI, Sagar DR, Ashraf S, Burston JJ, Suri S, Chapman V, et al. Differences in

- structural and pain phenotypes in the sodium monoiodoacetate and meniscal transection models of osteoarthritis. *Osteoarthritis Cartilage* 2013; 21: 1336-45.
49. Mapp PI, Walsh DA. Mechanisms and targets of angiogenesis and nerve growth in osteoarthritis. *Nat Rev Rheumatol* 2012; 8: 390-8.
  50. Nwosu LN, Allen M, Wyatt L, Huebner JL, Chapman V, Walsh DA, et al. Pain prediction by serum biomarkers of bone turnover in people with knee osteoarthritis: an observational study of TRAcP5b and cathepsin K in OA. *Osteoarthritis Cartilage* 2017; 25: 858-65.
  51. Walsh DA, Hu DE, Mapp PI, Polak JM, Blake DR, Fan TP. Innervation and neurokinin receptors during angiogenesis in the rat sponge granuloma. *Histochem J* 1996; 28: 759-69.
  52. Aso K, Ikeuchi M, Izumi M, Sugimura N, Kato T, Ushida T, et al. Nociceptive phenotype of dorsal root ganglia neurons innervating the subchondral bone in rat knee joints. *Eur J Pain* 2014; 18: 174-81.
  53. Aso K, Izumi M, Sugimura N, Okanoue Y, Ushida T, Ikeuchi M. Nociceptive phenotype alterations of dorsal root ganglia neurons innervating the subchondral bone in osteoarthritic rat knee joints. *Osteoarthritis Cartilage* 2016; 24: 1596-603.
  54. Jin Y, Smith C, Monteith D, Brown R, Camporeale A, McNearney TA, et al. CGRP blockade by galcanezumab was not associated with reductions in signs and symptoms of knee osteoarthritis in a randomized clinical trial. *Osteoarthritis Cartilage* 2018; 26: 1609-18.
  55. Chang YC, Lin WM, Hsieh ST. Effects of aging on human skin innervation. *Neuroreport* 2004; 15: 149-53.
  56. Karsdal MA, Michaelis M, Ladel C, Siebuhr AS, Bihlet AR, Andersen JR, et al. Disease-modifying treatments for osteoarthritis (DMOADs) of the knee and hip: lessons learned from failures and opportunities for the future. *Osteoarthritis Cartilage* 2016; 24: 2013-21.

**Figure 1: Histopathologic features in cartilage and subchondral bone from humans**

A; non-arthritic control. B; Asymptomatic chondropathy. C; Symptomatic chondropathy. Osteochondral channels were found in the subchondral bone plate in sections from non-arthritic control cases (D). Osteochondral channels breaching the tidemark and entering non-calcified cartilage in sections from symptomatic chondropathy cases (E). CGRP-IR nerves were found in osteochondral channels under the areas of damaged cartilage (asterisk) in sections from symptomatic chondropathy cases (white arrow head) (F, G). CGRP-IR sensory nerves (arrow) were found in bone marrow space (arrow) (H). (I)

explains where these images are located within the knee joint. Black arrow heads indicate tide mark. CGRP-IR; calcitonin gene-related peptide-immunoreactive. Scale bars = 100  $\mu\text{m}$

**Figure 2: Percentage of osteochondral channels containing CGRP-IR sensory nerves in non-arthritic control, symptomatic and asymptomatic chondropathy cases.**

Scatterplots illustrate the differences among non-arthritic control, symptomatic and asymptomatic chondropathy cases. Lines represent medians and IQR. Data were analysed using Kruskal-Wallis test followed by post hoc Dunn's comparison. \* $p=0.007$  versus asymptomatic chondropathy.

**Figure 3: Histopathologic features in cartilage and subchondral bone from rats**

A; Sham + vehicle. B; MNX + vehicle. C; MNX + AR786

Osteochondral channels (black arrow head) were found in the subchondral bone plate in sections from Sham + vehicle (A, D), MNX + vehicle (B, E) and MNX + AR786 group (C, F). CGRP-IR sensory nerves invading osteochondral channels from bone marrow space (white arrow head) under areas of damaged cartilage (asterisk) in MNX + vehicle group (G, H). The increase in CGRP-IR nerves within osteochondral channels under areas of damaged cartilage (asterisk) was prevented in MNX + AR786 group (I, J). CGRP-IR sensory nerves (arrow) were found in bone marrow space (K). MNX; meniscal transection, CGRP-IR; calcitonin gene-related peptide-immunoreactive. Scale bars = 100  $\mu\text{m}$

**Figure 4: Percentage of osteochondral channels containing CGRP-IR sensory nerves and nerve density in bone marrow space from sham plus vehicle, MNX plus vehicle and MNX plus AR786 models.**

Lines represent medians and IQR. \* $p=0.02$  versus Sham + vehicle and \* $p=0.03$  versus MNX + AR786. Data were analysed using Kruskal-Wallis test followed by post hoc Dunn's comparison. MNX; meniscal transection, CGRP; calcitonin gene-related peptide-immunoreactive, IR; immunoreactive.

	Non-arthritic control	Asymptomatic chondropathy	Symptomatic chondropathy
Age	50 (47, 65)	86 (78, 89)	61 (58, 73)
Gender (Male, %)	70	50	67



Macroscopic chondropathy score (0-100)	20 (17, 26)	68 (62, 83) *****	73 (66, 79) ****
Total radiographic OA severity score (0-18)	NA	NA	12 (10.5, 13)
Tibiofemoral JSN score (0-6)	NA	NA	5 (5, 5)
Medial tibiofemoral JSN score (0-3)	NA	NA	3 (3, 3)
Osteophyte score (0-12)	NA	NA	7 (5.5, 8)
Medial tibial osteophyte score (0-3)	NA	NA	2 (1.5, 2)
Total Mankin score (0-14)	6 (5, 8)	9 (6, 11)	11 (9, 12) *
Loss of cartilage surface integrity (0-6)	3 (2, 3)	5 (3, 6) ***	6 (4, 6) **
Chondrocyte appearance (0-3)	2 (2, 3)	3 (3, 3)	3 (3, 3)
Loss of tidemark integrity (Yes, %)	45	70	70
Proteoglycan loss (0-4)	1 (1, 1)	2 (1, 2)	2 (2, 2)
Subchondral bone marrow replacement (Yes, %)	45	67	64
Density of channels breaching tidemark (/mm)	0.00 (0.00, 0.00)	0.03 (0, 0.10)	0.07 (0.00, 0.13)
Total osteochondral channel density (/mm)	4.4 (3.9, 4.7)	3.7 (3.0, 5.0)	4.1 (3.3, 6.6)

**Table 1: Details of demographics, radiographic OA severity and OA pathology**

Data displayed as median (IQR). Total radiographic OA severity score is a summation of tibiofemoral joint space narrowing (JSN) and osteophyte scores. Tibiofemoral JSN score is a summation of medial and lateral tibiofemoral JSN scores. Osteophyte score is a summation of medial and lateral tibial and femoral osteophyte scores. Data were analysed using Kruskal-Wallis test followed by post hoc Dunn's comparison. \*p=0.01, \*\*p=0.007, \*\*\*p=0.006, \*\*\*\*p=0.003, \*\*\*\*\*p=0.0002 versus non-arthritis control. JSN; joint space narrowing, NA = Not available.

	SHAM + Vehicle	MNX + Vehicle	MNX + AR786
Macroscopic chondropathy score	0 (0, 0.8)	3 (3, 3)**	3 (3, 4)****
Cartilage damage score (0-15)	0 (0, 0)	5 (3, 8)	6 (5, 10)*
Osteophyte score (0-3)	0 (0, 0)	1 (0, 3)	1 (0, 2)
Osteochondral channel density (/mm)	3.1 (2.9, 3.3)	2.5 (2.2, 3.6)	3.5 (2.5, 4.6)
Subchondral bone marrow replacement (%)	0	50	66.7*
Paw withdrawal threshold (g)	15 (11, 15)	6 (5, 6)***, #	13 (10, 15)
Weight-bearing asymmetry (%)	1.2 (0.1, 1.9)	25.2 (20.6, 27.4)***, ##	1.5 (0.6, 3.8)

**Table 2: Histology and pain behavior 28 days after knee surgery in rats**

Data displayed as median (IQR) and 95% confidence interval (CI) for median. Data were analysed using Kruskal-Wallis test followed by post hoc Dunn's comparison. \*p=0.003, \*\*p=0.002, \*\*\*p=0.0001, \*\*\*\*p<0.0001 versus SHAM+Vehicle. #p=0.003, ##p=0.002 versus MNX + AR786. MNX; meniscal transection. Weight-bearing asymmetry is given as percent difference in distribution between hindlimbs.

¥; Macroscopic chondropathy score, paw withdrawal threshold and weight-bearing asymmetry have been previously published<sup>8</sup>.

### Supplementary text

#### Method of Zamboni<sup>23</sup>

Samples were fixed using a solution of 2% (w/v) paraformaldehyde, 15% (v/v) picric acid in phosphate buffer (pH 7.3, 4°C) overnight, and then transferred to 15% (w/v) sucrose in phosphate buffered saline (4°C) solution for 5 days.

#### Mankin scoring system<sup>26</sup>

Cartilage surface integrity (0 [normal] to 6 [complete disorganisation]), tidemark integrity (0 [intact] or 1 [crossed by vessels]), chondrocyte morphology (0 [normal] to 3 [hypocellular]) and proteoglycan loss (0 [normal, no loss of Safranin-O stain] to 4 [complete loss of stain]).

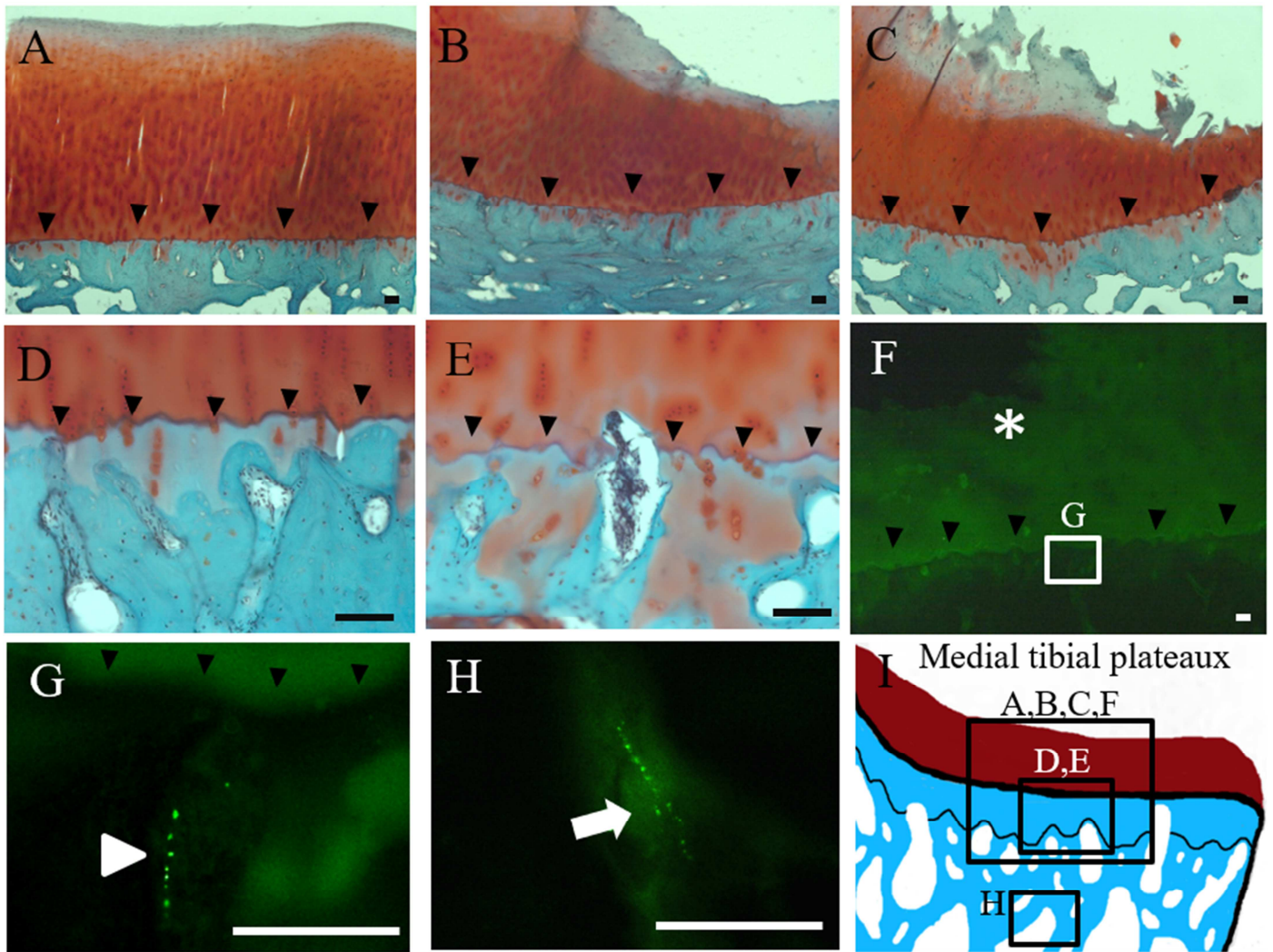
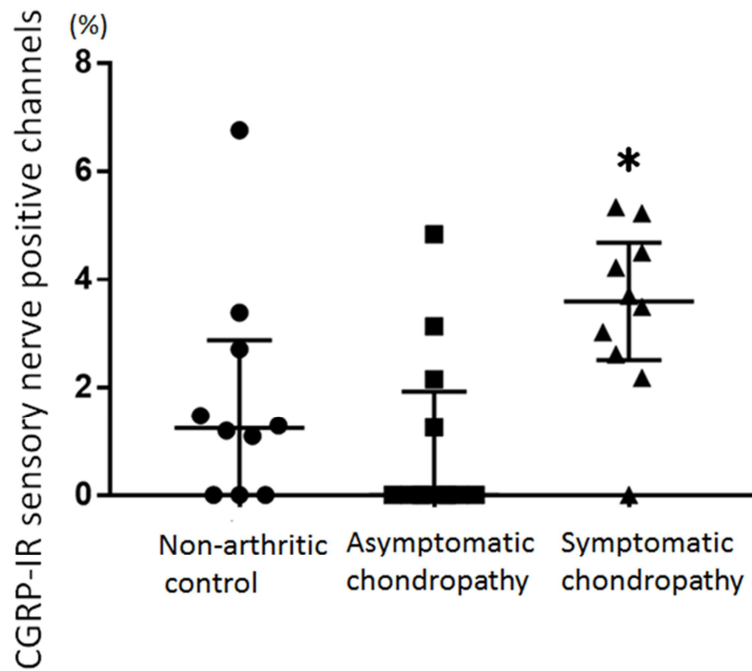
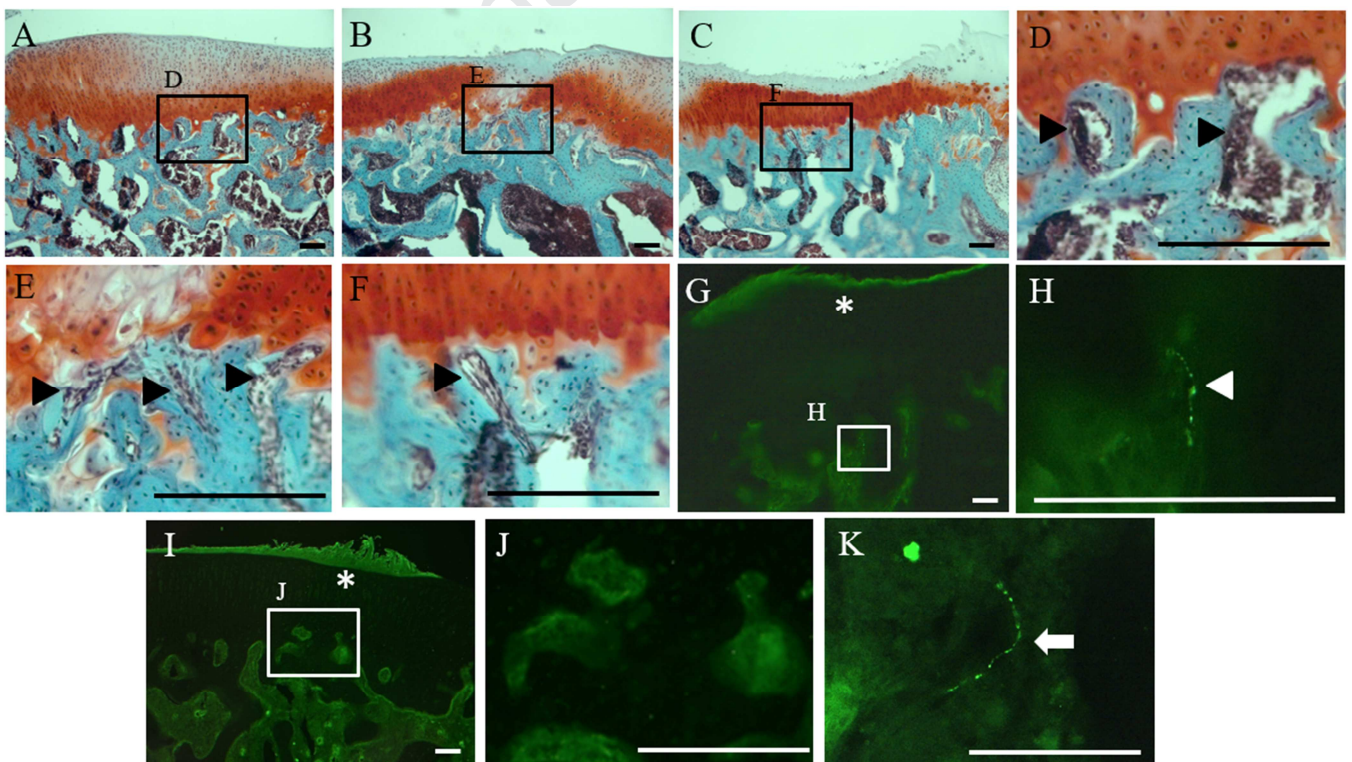


Figure 1: Histopathologic features in cartilage and subchondral bone from humans



**Figure 2: Percentage of osteochondral channels containing CGRP-IR sensory nerves in non-arthritic control, symptomatic and asymptomatic chondropathy cases.**



**Figure 3: Histopathologic features in cartilage and subchondral bone from rats**

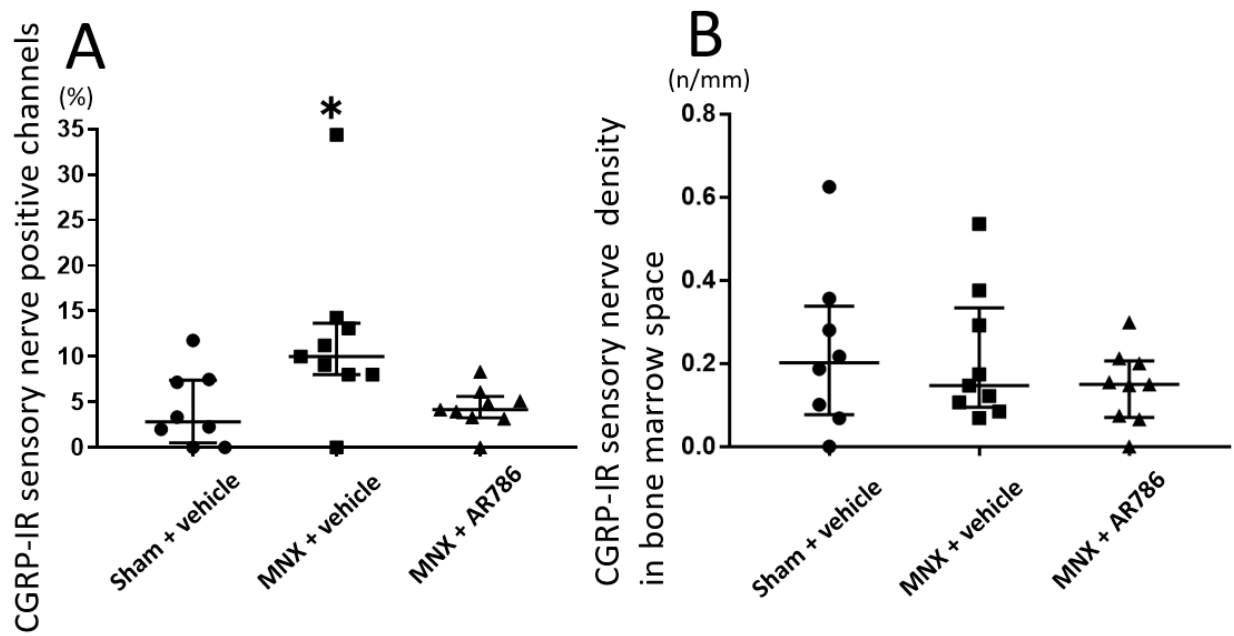


**Figure 4: Percentage of osteochondral channels containing CGRP-IR sensory nerves and nerve density in bone marrow space from sham plus vehicle, MNX plus vehicle and MNX plus AR786 models.**